Quenching the collective effects on the two-photon correlation from two double-Raman atoms

C. H. Raymond Ooi*
Max-Planck-Institut für Quantenoptik, D-85748, Garching, Germany
and Department of Physics, Korea Advanced Institute of Science and Technology, Daejeon 305-701, Republic of Korea
(Received 26 January 2007; published 26 April 2007)

We obtain an analytical expression for two-photon correlation $G^{(2)}$ from two atoms driven in a double-Raman (or Λ) configuration where collective effects such as superradiant, subradiant, and dipole-dipole interaction are included. It is found that the collective effects on the $G^{(2)}$ can be quenched to some extent by a resonant control laser field. The collective effects provide features via $G^{(2)}$ that enable the two atoms to be resolved at subwavelength separation. We also identify an effect in the double Raman scheme due to the collective effects and the control field, i.e., the Stokes and anti-Stokes frequencies are increased by fourfold.

DOI: 10.1103/PhysRevA.75.043817 PACS number(s): 42.50.Fx, 42.50.Ar, 32.80.−t, 42.65.Ky

I. INTRODUCTION

It is known that correlated multiphoton detection scheme enhances the resolving power of two point sources, for example, by using Glauber's two-photon correlation $G^{(2)}$ [1]. Subwavelength resolution using interference of classical thermal light has recently been reported [2]. Nonclassical light is also capable of providing an enhancement factor. In particular, the Raman-EIT (electromagnetic induced transparency) scheme (Fig. 1) which shows photon antibunching and quantum interference [3] can be used to resolve two atoms as close as $\lambda/8$ by measuring the two-photon correlation in an interferometric setup [5]. However, at subwavelength distance, the presence of *collective* phenomena (superradiant and subradiant) via *dipole-dipole interaction* due to vacuum fields [6] may invalidate the approximate analysis based on the summing of two-photon amplitudes $\psi_j(j=1,2)$ of two independent atoms, i.e., $\psi_1+\psi_2$. The two-atom system (of Fig. 1) must be solved as a whole, taking into account the collective many-particle radiation states.

The main purpose of this paper is to study the physics of the $G^{(2)}$ in the simplest driven collective many-body system that produces *nonclassically correlated* photon pairs. A particularly interesting question is, how does the coexistence of the dipole-dipole interaction and the control field in the Raman-EIT scheme affect the two-photon correlation? The $G^{(2)}$ for a single atom with Raman-EIT scheme has been studied by various methods [7]. It is convenient to use the Schrödinger's equation approach [4] to obtain an analytical expression for the $G^{(2)}$ that would facilitate physical interpretations.

We shall focus our discussions of the physics around small interatomic distance r. We show how the collective effects of dipole-dipole interaction can be quenched by a control field. We also find that $G^{(2)}$ as a function of time delay τ between the Stokes and anti-Stokes photons contains features due to the dipole-dipole interaction that enable the two atoms at subwavelength distance to be resolved without using the interferometric setup.

*Email address; bokooi73@yahoo.com

II. TWO-ATOM DYNAMICS

The interaction Hamiltonian for two independent (*noninteracting*) Raman-EIT atoms in free space radiation and driven by two laser fields (Fig. 1) in the interaction picture is simply the independent sum of two Hamiltonians, each for a single atom,

$$\hat{V} = -\hbar\Bigg[\sum_{j=1,2,\mathbf{k}} G_{\mathbf{k}}^{(j)}\hat{a}_{\mathbf{k}}^{\dagger}|b_j\rangle\langle c_j|e^{-i\Delta t}e^{i\Delta_{\mathbf{k}}t} + \Omega_c^{(j)}e^{-i\delta t}|a_j\rangle\langle b_j| + \sum_{\mathbf{q}} g_{\mathbf{q}}^{(j)}\hat{a}_{\mathbf{q}}^{\dagger}|c_j\rangle\langle a_j|e^{i\Delta_{\mathbf{q}}t} + \text{adj}\Bigg]. \quad (1)$$

Each Hamiltonian describes a single Raman-EIT atom [3], the $G_{\mathbf{k}}^{(j)}=g_{\mathbf{k}}^{(j)}\Omega_p^{(j)}/\Delta$ is the spontaneous Raman coupling, $\Omega_p^{(j)}(<<\Delta)$ and $\Omega_c^{(j)}$ are the Rabi frequencies of the jth atom coupled to the far detuned weak pump laser that drives the $c\leftrightarrow d$ transition and the control laser that drives the $b\leftrightarrow a$ transition, respectively, $g_{\mathbf{k}}^{(j)}=-(\vec{\wp}\cdot\hat{\varepsilon}_{\mathbf{k}}^{*})_{bd}\sqrt{\frac{\omega_{\mathbf{k}}}{2\varepsilon_o\hbar V}}e^{-i\mathbf{k}\cdot\mathbf{r}_j}$ and $g_{\mathbf{q}}^{(j)}=-(\vec{\wp}\cdot\hat{\varepsilon}_{\mathbf{q}}^{*})_{ca}\sqrt{\frac{\omega_{\mathbf{q}}}{2\varepsilon_o\hbar V}}e^{-i\mathbf{q}\cdot\mathbf{r}_j}$ are the couplings of the radiation to the $b\leftrightarrow d$ transition and the $c\leftrightarrow a$ transition, respectively, $\mathbf{r}_j$ denotes the position of the jth atom, and $\Delta_{\mathbf{k}(\mathbf{q})}=\nu_{\mathbf{k}(\mathbf{q})}-\omega_{db(ac)}$ with $\Delta=\nu_p-\omega_{dc}$ are the detunings.

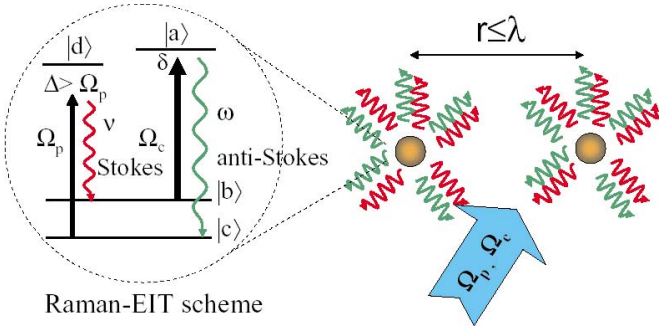

FIG. 1. (Color online) Two atoms driven by a pump laser and a control laser with Rabi frequencies Ω_p and Ω_c, respectively, in the Raman-EIT scheme. Correlated photon pairs, called Raman emission doublet (RED) are emitted. The atoms are separated by a distance r which can be close to the emission wavelength $\lambda \doteq 2\pi c/\omega \simeq 2\pi c/\nu$.

We consider a sufficiently weak pump field such that states with two and more Stokes photons are negligible. Thus, the collective two-atom-radiation state vector is

$$|\Psi(t)\rangle = C|c_1,c_2,0\rangle + \sum_{\mathbf{k}} \{B_{\mathbf{k}}^{(1)}|b_1,c_2\rangle + B_{\mathbf{k}}^{(2)}|c_1,b_2\rangle\}|1_{\mathbf{k}}\rangle + \sum_{\mathbf{k}} \{A_{\mathbf{k}}^{(1)}|a_1,c_2\rangle + A_{\mathbf{k}}^{(2)}|c_1,a_2\rangle\}|1_{\mathbf{k}}\rangle + \sum_{\mathbf{k},\mathbf{q}} C_{\mathbf{k},\mathbf{q}}(t)|c_1,c_2,1_{\mathbf{k}},1_{\mathbf{q}}\rangle, \tag{2}$$

where C, $B_{\mathbf{k}}^{(j)}$, $A_{\mathbf{k}}^{(j)}$, and $C_{\mathbf{k},\mathbf{q}}$ are the probability amplitudes for the collective basis states: (i) both atoms in c with no photon, (ii) one of the atoms driven to b by spontaneous Raman process, and (iii) coherently coupled to a with the emission of a Stokes photon $\mathbf{k}$, and (iv) the same atom that emits photon $\mathbf{k}$ decays to level c emitting an anti-Stokes photon $\mathbf{q}$. Note that the intermediate states b and a are *entangled*; we know only one is excited but never know *which one*.

The Schrödinger's equation gives a set of coupled equations for the coefficients C, $B_{\mathbf{k}}^{(j)}$, $A_{\mathbf{k}}^{(j)}$, and $C_{\mathbf{k},\mathbf{q}}$ that are solved in Appendix using standard procedure [4]. As shown in the Appendix, the above Hamiltonian and state vector automatically give rise to the $f(r)$ function [see Eq. (A8)] which accounts for the dipole-dipole interaction, without introducing any Hamiltonian to describe the direct interaction between the two atoms. Here, the dipole-dipole interaction is indirect, mediated by the vacuum radiation.

III. COLLECTIVE TWO-PHOTON AMPLITUDE

In order to compute the two-photon correlation $G^{(2)} = |\psi_{\mathrm{RED}}(B,A) + \psi_{\mathrm{RED}}(A,B)|^2$, the steady state solution for $C_{\mathbf{k},\mathbf{q}}$, i.e., Eq. (A9) is used. After lengthy calculations involving pole integrations [9], we obtain the two-photon amplitude as the main result

$$\psi_{\mathrm{RED}}(B,A) = \sum_{j=1,2} [\{\psi_+^{(+)}(Bj,Aj) - \psi_-^{(+)}(Bj,Aj)\} - \{\psi_+^{(-)}(Bj,Aj) - \psi_-^{(-)}(Bj,Aj)\}] - \frac{1}{2}[\{\psi_+^{(+)}(B2,A1) - \psi_-^{(+)}(B2,A1)\} - \{\psi_+^{(-)}(B2,A1) - \psi_-^{(-)}(B2,A1)\} + (1-2)], \tag{3}$$

where $(\pm)$ are the signs for superradiant $(+)$ and subradiant $(-)$ cases, with the partial amplitudes

$$\psi_{\pm}^{(\pm)}(Bj,Aj) = -\frac{C_j}{2\tilde{\Omega}^{(\pm)}}\Theta(\tau_{Aj})\left\{(\pm)\frac{1}{2}e^{-\{i(\nu' \mp \tilde{\Omega}^{(\pm)}) + [\gamma_R - (1/4)\Gamma^{(\pm)}]\}\tau_{Aj}}e^{-[i(\omega' \pm \tilde{\Omega}^{(\pm)}) + (1/4)\Gamma^{(\pm)}]\tau_{Bj}}\Theta(\tau_{BjAj}) + \frac{|\Omega_c|^2}{i\Gamma f(r)\left(\frac{1}{2}\delta + i\frac{1}{4}\Gamma^{(\pm)} \mp \tilde{\Omega}^{(\pm)}\right)}e^{-i\nu\tau_{Aj}}e^{-i\omega\tau_{Bj}}e^{-\gamma_R\tau_{Aj}}\right\}, \tag{4}$$

$$\psi_{\pm}^{(\pm)}(B2,A1) = \frac{C_{21}}{2\tilde{\Omega}^{(\pm)}}\Theta(\tau_{A1})e^{-\{i(\nu' \mp \tilde{\Omega}^{(\pm)}) + [\gamma_R - (1/4)\Gamma^{(\pm)}]\}\tau_{A1}}e^{-[i(\omega' \pm \tilde{\Omega}^{(\pm)}) + (1/4)\Gamma^{(\pm)}]\tau_{B2}}\Theta(\tau_{B2} - \tau_{A1}), \tag{5}$$

where $\nu' \doteq \nu + \frac{1}{2}\delta$ and $\omega' \doteq \omega - \frac{1}{2}\delta$ are the effective Stokes and anti-Stokes frequencies with $\nu \doteq \nu_p - \omega_{bc}, \omega \doteq \nu_c + \omega_{bc} = \delta + \omega_{ac}$; $\tau_{BjAj} = \tau_{Bj} - \tau_{Aj}$; and $\tau_{Aj} = t_A - r_{Aj}/c, \tau_{Bj} = t_B - r_{Bj}/c$ are the retarded times. The physical significance of each term in Eq. (3) is illustrated in Fig. 2. The coefficients are

$$C_j = -\frac{(\nu\omega/c^2)^3}{(4\pi\varepsilon_o)^2}\frac{\Omega_p}{\Delta}\Omega_c K_{Aj} Q_{Bj} e^{i(\mathbf{k}_c + \mathbf{k}_p)\cdot\mathbf{r}_j}, \tag{6}$$

$$C_{21} = -\frac{(\nu\omega/c^2)^3}{(4\pi\varepsilon_o)^2}\frac{\Omega_p}{\Delta}\Omega_c K_{A1} Q_{B2} e^{i\mathbf{k}_c\cdot\mathbf{r}_2} e^{i\mathbf{k}_p\cdot\mathbf{r}_1}, \tag{7}$$

and the effective complex Rabi frequencies that contain the collective effects (via $\Gamma^{(\pm)}$) and the ac Stark shift (via Ω_c) are

$$\tilde{\Omega}^{(\pm)} = \sqrt{\Omega_c^2 - \left(\tfrac{1}{4}\Gamma^{(\pm)} - i\tfrac{1}{2}\delta\right)^2}. \tag{8}$$

The coherent phases $\mathbf{k}_q\cdot\mathbf{r}_j = k_q r_j \cos\alpha_q$ $(q = p, c)$ give rise to an additional interference feature shown in Fig. 3. The $\Gamma^{(\pm)} = \Gamma[1 \pm f(r)]$ in Eqs. (4), (5), and (8) are complex; where $f(r) = g(r) + ih(r)$ is the dimensionless collective parameter that includes the modified collective (subradiant and superradiant) decay rate factor $g(r)$ and the vacuum-induced coherent dipole-dipole interaction factor $h(r)$. Full expressions for $g(r), h(r)$ are well known and can be found, for example in [6,8], but we reproduce them in Fig. 4(c) for convenience. For sufficiently large interatomic distance: $\omega r/c, \nu r/c \gg 1$, we have negligible collective effects since $f(r) \to 0$.

Note that for sufficiently weak field $\Omega_c \ll \Gamma$, Eq. (8) gives $\tilde{\Omega}^{(\pm)} \simeq i\frac{1}{4}\Gamma^{(\pm)} + \frac{1}{2}\delta$. Here, the real part $\frac{1}{2}\delta \mp \frac{1}{4}\Gamma h$ simulates the role of Rabi frequency. This indicates the contributions of the collective (two atom) effect, namely the vacuum induced coherent dipole-dipole interaction, and finite laser detuning δ to the coherent quantum phenomena such as Rabi oscillations,

and nonclassical effect (photon antibunching), as shown in Fig. 3. In the limit of large atomic separation, the cooperative effects vanish since $f(r)\to 0$ and taking $\delta=0$ we find $\Omega_{\pm}^{(\pm)} \simeq \pm\tilde{\Omega}$ where $\tilde{\Omega}=\sqrt{\Omega_c^2-(\Gamma/4)^2}$. Then, $\psi_{\pm}^{(-)}(Bj,Aj)\simeq -\psi_{\pm}^{(+)} \times(Bj,Aj)$ and Eq. (3) reduces to the sum of amplitudes of two independent atoms [3,9],

$$\psi_{\mathrm{RED}}(B,A) \simeq \sum_{j=1,2} \frac{C_j}{2\tilde{\Omega}}[e^{i\tilde{\Omega}(\tau_{Bj}-\tau_{Aj})} - e^{-i\tilde{\Omega}(\tau_{Bj}-\tau_{Aj})}] \times\Theta(\tau_{Bj}-\tau_{Aj})e^{-(i\nu'+\gamma_R)\tau_{Aj}}e^{-i\omega'\tau_{Bj}}e^{-(1/4)\Gamma(\tau_{Bj}-\tau_{Aj})}. \tag{9}$$

Here, Eq. (9) corresponds to the asymmetrical emission paths shown in Fig. 2(a). The symmetrical paths of Fig. 2(b) do not contribute since the paths that correspond to the subradiant [superscript $(-)$] cancel those paths for the superradiant [superscript $(+)$].

IV. COHERENT CONTROL VIA COLLECTIVE EFFECTS

The essence of this paper can be found in the complex Rabi frequency $\tilde{\Omega}^{(\pm)}$ and we discuss how the field dependence modifies the frequency components, Rabi oscillations and decay rates.

A. Multiple frequencies

The amplitude Eq. (9) for large r has simple meaning: the Stokes photon with frequency ν' is emitted at an emission time τ_{Aj} with probability $\exp\{-\gamma_R\tau_{Aj}\}$ from the jth atom and goes to detector A, the anti-Stokes photon with frequency ω' is emitted at an emission time τ_{Bj} with the probability $\exp\{-\frac{1}{4}\Gamma(\tau_{Bj}-\tau_{Aj})\}$ from the jth atom and goes to detector B.

The general amplitude equations (3)–(5) can be interpreted similarly. Thus, we find that the real part $\mathrm{Re}\,\tilde{\Omega}^{(\pm)}$ and the imaginary part of $\Gamma^{(\pm)}$ give the eight possible frequency components: $\nu'\mp\mathrm{Re}\,\tilde{\Omega}^{(\pm)}(\mp)\frac{1}{4}h\Gamma$ for Stokes photon and $\omega'\pm\mathrm{Re}\,\tilde{\Omega}^{(\pm)}(\pm)\frac{1}{4}h\Gamma$ for anti-Stokes photon. These frequencies give rise to the various possible interfering paths shown in Fig. 2. Clearly, the frequency sidebands are due to Rabi splitting and dipole-dipole interaction. As found in Fig. 4(a), the distinction between these lines increase for small r and large Ω_c.

These are real frequencies that can be obtained by calculating the power spectrum via the field correlation $\langle E^{\dagger}(t+\tau)\hat{E}(t)\rangle$. Of course, they would not show up in the correlated measurement of the $G^{(2)}$. Only the beats among the frequencies are found if we make a Fourier transformation of the $G^{(2)}$. It is essentially the beats (due to the dipole-dipole interaction) that were used for subwavelength measurement of two atoms in Ref. [10].

We expect that a larger number of atoms would give a larger number of sidebands. This could be an alternative method to nonlinear optical processes for the generation of multiple new frequencies. We shall not pursue this further here since it is not the main focus and beyond the present scope. Further analysis will be reported elsewhere.

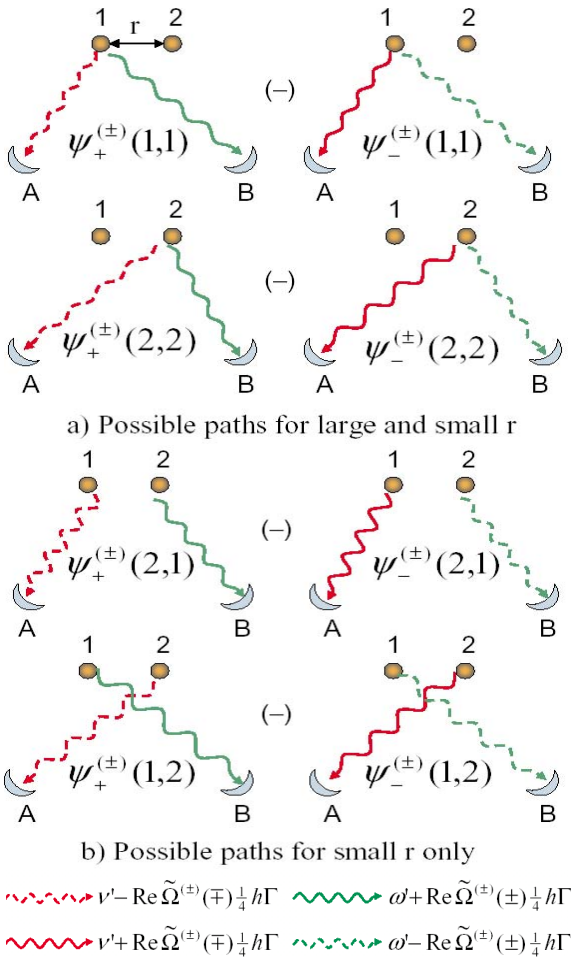

FIG. 2. (Color online) Possible (a) asymmetrical and (b) symmetrical emission paths based on the result of two photon amplitude, Eq. (3) [red (dark) lines: for Stokes; green (light) lines: for anti-Stokes; solid lines: for $\cdots+\mathrm{Re}\,\tilde{\Omega}^{(\pm)}\cdots$, dashed lines: for $\cdots-\mathrm{Re}\,\tilde{\Omega}^{(\pm)}\cdots$.] Note that Eq. (3) also predicts the existence of eight frequency sidebands, i.e., a fourfold increase in the number of frequencies due to Autler-Townes splitting by the control field Ω_c and dipole-dipole interaction, as shown below (b).

B. Rabi oscillations and threshold

The Rabi oscillation period is governed by the real part of $\tilde{\Omega}^{(\pm)}$, particularly by the control field Ω_c, g, and h. Figures 4(a) and 4(b) show $\tilde{\Omega}^{(\pm)}$ as a function of r in two perspectives. There is a threshold Ω_{thr} for transition between overdamp ($\Omega_c<\Omega_{\mathrm{thr}}$) and oscillatory ($\Omega_c<\Omega_{\mathrm{thr}}$) regimes. For large r, the threshold is clearly seen around $\frac{1}{4}\Gamma$ (as in single atom case) in Fig. 4(b). If h can be neglected and $\delta=0$, we have $\Omega_{\mathrm{thr}}\simeq\frac{1}{4}\Gamma(1+g)$. The overdamp and oscillatory regimes are well defined by hyperbolic and trigonometric functions, respectively, only when $\tilde{\Omega}^{(\pm)}$ are either real or purely imaginary. As r decreases h becomes significant, the argument inside $\sqrt{\cdots}$ of Eq. (8) becomes complex and there is no simple analytical expression for the threshold.

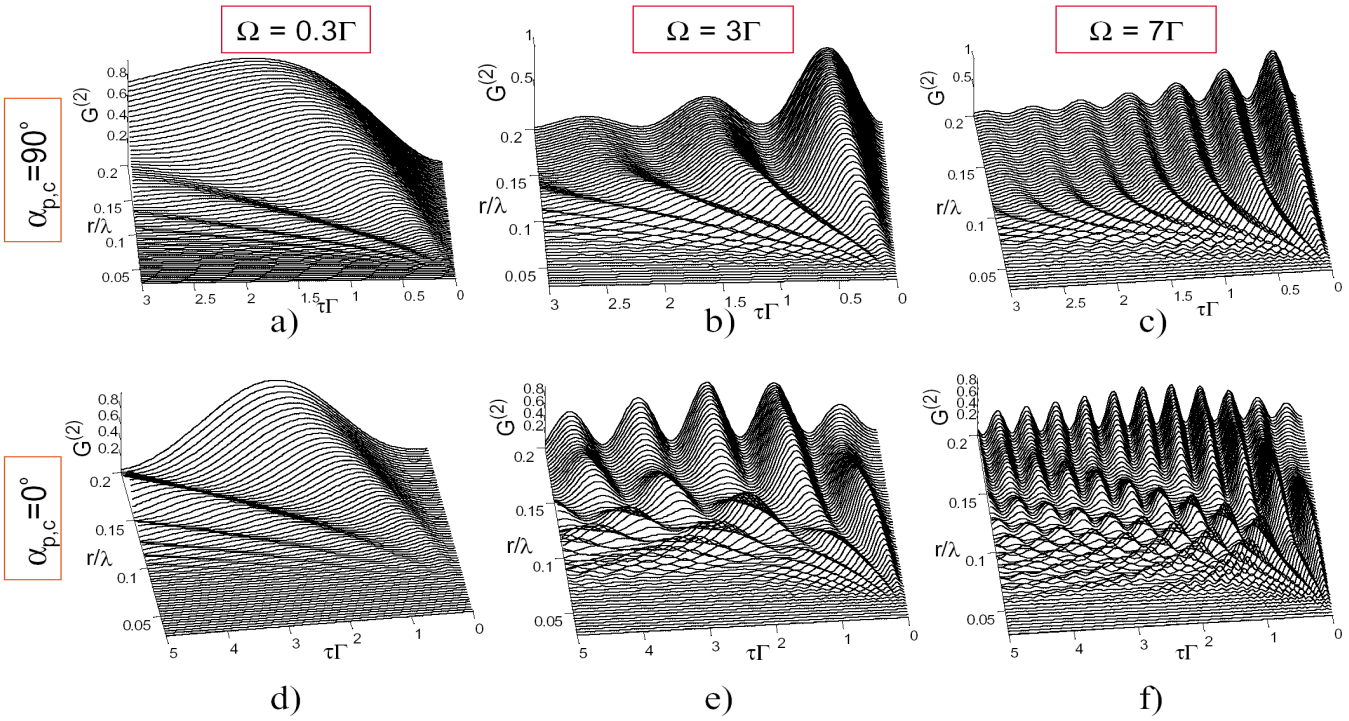

FIG. 3. (Color online) Plots of two-photon correlation (normalized) in the regime where dipole-dipole interaction is significant for $\alpha_c = \alpha_p = 90°$ with different control fields (a) $\Omega_c = 0.2\Gamma$ corresponds to overdamp regime in the limit of large r, (b) $\Omega_c = 3\Gamma$, and (c) $\Omega_c = 7\Gamma$, and for $\alpha_c = \alpha_p = 0°$ (with the same set of control fields) which gives the interference effect of the coherent phase factor $e^{i(\mathbf{k}_p+\mathbf{k}_c)\cdot\mathbf{r}_j}$. Note that the onset to a more rapid Rabi oscillation in each plot is dependent on Ω_c. This feature can be understood by looking at Fig. 4. We have considered parallel transitions $\Delta M = 0$ (with identical results for $\Delta M = \pm 1$). For simplicity, we take $\delta = 0$. The results are independent of the angle α_{Dj} between the photon from atom j to detector D and the interatomic axis.

C. Multiple decay rates

Since $\Gamma^{(\pm)}$ is complex, Eq. (2) shows that there are eight effective decay rates governed by $\exp(\{\frac{1}{4}\Gamma[1(\pm)g] \mp \mathrm{Im}\,\tilde{\Omega}^{(\pm)} - \gamma_R\}\tau_{Aj})$ for the Stokes photon and $\exp(\{\frac{1}{4}\Gamma[1(\pm)g] \mp \mathrm{Im}\,\tilde{\Omega}^{(\pm)}\}\tau_{Bj})$ for the anti-Stokes photon. At $r = n\lambda/2$ where $n = 1, 2, 3, \ldots$. we find that the value of $\mathrm{Im}\,\tilde{\Omega}^{(\pm)}$ jumps from positive to negative or otherwise for Ω_c below Ω_{thr}. Since the imaginary part of $\tilde{\Omega}^{(\pm)}$ also depends on Ω_c, the laser field also affects the multiple decay rates. Thus, the laser field not only modifies the Rabi oscillations in the $G^{(2)}$ but also its damping rate as a function of τ.

V. RESULTS OF THE CORRELATION

By using filters at the detectors such that detector A detects photon ν and B detects photon ω, the term $\psi_{\mathrm{RED}}(A, B)$

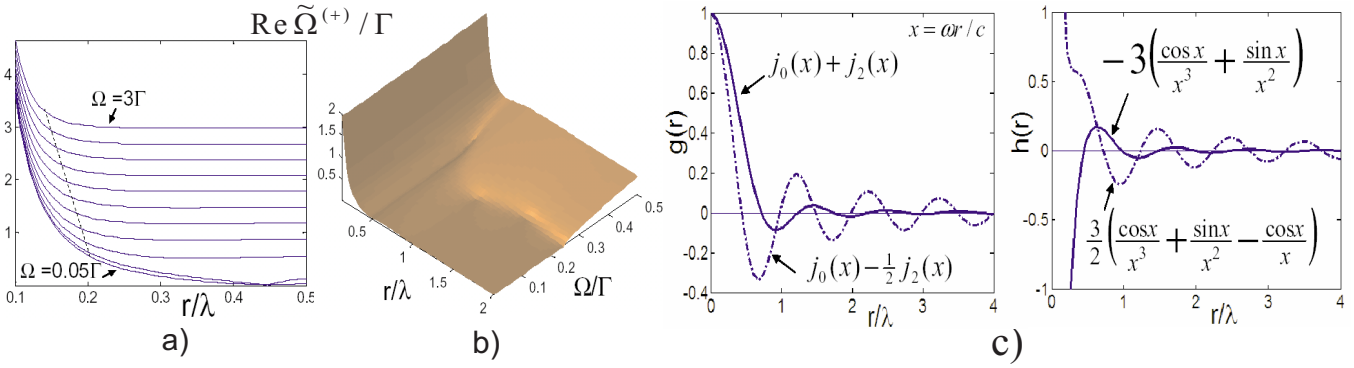

FIG. 4. (Color online) (a) The real part of $\tilde{\Omega}^{(+)}$ [from Eq. (8)] for Ω_c from 0.05Γ to 3Γ for $\Delta M = 0$. The dashed line estimates the turning points r_t of the curves with different Ω_c. (b) The $\mathrm{Re}\,\tilde{\Omega}^{(+)}$ versus r and Ω_c. The kink points close to $r = \lambda$, $\lambda/2$, and $3\lambda/2$ correspond to the zeros of the h function. The points where $\mathrm{Re}\,\tilde{\Omega}^{(+)} = 0$ correspond to the transition between overdamp and oscillatory regimes. Similar features are found for $\tilde{\Omega}^{(-)}$. (c) $g(r)$ and $h(r)$ for parallel transition $\Delta M = 0$ (solid line) and perpendicular $\Delta M = \pm 1$ (dashed-dotted line), ΔM is the change in magnetic quantum number, j_n is spherical Bessel of order n.

obtained by interchanging A with B in Eq. (3) can be disregarded. Figure 3 shows the variations of $G^{(2)}(r,\tau)=|\psi_{\mathrm{RED}}(r,\tau)|^2$ as a function of detection time delay $\tau=t_B-t_A$ between Stokes and anti-Stokes and interatomic distance r.

Collective effects on $G^{(2)}$. The collective effect on the $G^{(2)}$ profile becomes significant when the period of oscillations varies appreciably around some transition (or turning) point referred to as r_t, which can only be estimated subjectively. Typically $r_t<\lambda$. For $r<r_t$, the dipole-dipole interaction dominates and causes the Rabi oscillations to become more rapid. In this regime, the correlation can be oscillatory even when $\Omega_c<\Gamma/4$ (overdamp for large r); as in the case of $\Omega_c=0.3\Gamma$ in Fig. 3(a). However, the magnitude of the correlation decreases for $r<r_t$, since the atoms are more likely to exchange photons between each other (Rabi oscillations via emission and reabsorption) instead of emitting photons to the environment (dissipation).

Quenching effect of control field. By comparing the plots for several values of the control field Ω_c in Fig. 3, we find that r_t becomes smaller as Ω_c increases. This shows the *quenching* of the effect of dipole-dipole interaction by the control field. This feature is supported by Fig. 4(a) (Re $\tilde{\Omega}^{(+)}$ versus r) which shows the variation of the estimated turning points r_t for different Ω_c (visually guided by the dashed line). For larger Ω_c, the Re $\tilde{\Omega}^{(+)}$ increases drastically around smaller values of r_t, which corresponds to Fig. 3(c). For small Ω_c the Rabi oscillation period begins to change significantly only at the larger r_t, which corresponds to Fig. 3(a). For $\Omega_c=3\Gamma$ Fig. 3(b) shows that the sum of amplitudes of two independent atoms $G^{(2)}\simeq|\psi_{\mathrm{RED1}}+\psi_{\mathrm{RED2}}|^2$ is a good approximation down to $\lambda/8$, thus the analysis of Ref. [5] which employs this approximation to achieve a resolution up to $\lambda/8$ is valid.

Coherent phase of lasers. When $\alpha_{p,c}\neq\pi/2$, the coherent phase factors $e^{i\mathbf{k}_{p,c}\cdot\mathbf{r}_j}$ in Eqs. (6) and (7) give richer features shown in Figs. 3(d)–3(f). For large r, the oscillations across r become more rapid. Similarly for small r, but the oscillations also become more rapid across τ. The wave vectors of the lasers introduce a relative phase (that depends on r) between the two atoms such that their transient dynamics evolve out of phase between each other and this creates the beating.

Subwavelength resolution. The variation of the Rabi oscillations period in the $G^{(2)}$ with r (due to collective effect) is a feature that can be used to measure the interatomic distance r below the diffraction limit of the photons. One should realize that this feature is in time domain, in contrast to the approach using the frequency domain [10] although the physics is the same. Besides, the resolution may be limited by the vanishingly small correlation for $r\lesssim\lambda/20$. Further analysis of the $G^{(2)}$ as a function of τ and its Fourier transform for subwavelength resolution will be reported elsewhere.

In conclusion, the significance of the above results is that the collective effects at small interatomic distance give rise to distance dependent two-photon correlation that can be "quenched" by a strong resonant control field Ω_c. This provides a possibility of coherently controlling the collective photon statistics and multiple frequency generation in the many-body system.

ACKNOWLEDGMENT

The author thanks Professor Iwo Bialynicki Birula for helpful feedback that led to this work.

APPENDIX: COUPLED EQUATIONS AND SOLUTIONS

The coupled equations for two RED atoms obtained from Eqs. (1) and (2) are

$$\frac{d}{dt}C=i\sum_{\mathbf{k}}(G_{\mathbf{k}}^{(1)*}\tilde{B}_{\mathbf{k}}^{(1)}+G_{\mathbf{k}}^{(2)*}\tilde{B}_{\mathbf{k}}^{(2)}), \tag{A1}$$

$$\left(\frac{d}{dt}+iD_{\mathbf{k}}\right)\tilde{B}_{\mathbf{k}}^{(j)}=iG_{\mathbf{k}}^{(j)}C+i\Omega_c^{(j)*}\tilde{A}_{\mathbf{k}}^{(j)}, \tag{A2}$$

$$\left(\frac{d}{dt}+i(D_{\mathbf{k}}-\delta)\right)\tilde{A}_{\mathbf{k}}^{(j)}=i\Omega_c^{(j)}\tilde{B}_{\mathbf{k}}^{(j)}+i\sum_{\mathbf{q}}g_{\mathbf{q}}^{(j)*}\tilde{C}_{\mathbf{k},\mathbf{q}}, \tag{A3}$$

$$\left(\frac{d}{dt}+iD_{\mathbf{k},\mathbf{q}}\right)\tilde{C}_{\mathbf{k},\mathbf{q}}=ig_{\mathbf{q}}^{(1)}\tilde{A}_{\mathbf{k}}^{(1)}+ig_{\mathbf{q}}^{(2)}\tilde{A}_{\mathbf{k}}^{(2)}, \tag{A4}$$

where $j=1,2$ and we define the transformation

$$\tilde{B}_{\mathbf{k}}^{(j)}=B_{\mathbf{k}}^{(j)}e^{i\Delta t}e^{-i\Delta_{\mathbf{k}}t},$$

$$\tilde{A}_{\mathbf{k}}^{(j)}=A_{\mathbf{k}}^{(j)}e^{i\Delta t}e^{-i\Delta_{\mathbf{k}}t}e^{i\delta t},$$

$$\tilde{C}_{\mathbf{k},\mathbf{q}}=C_{\mathbf{k},\mathbf{q}}e^{i\Delta t}e^{-i\Delta_{\mathbf{k}}t}e^{i\delta t}e^{-i\Delta_{\mathbf{q}}t}$$

with the detunings

$$D_{\mathbf{k}}=\Delta_{\mathbf{k}}-\Delta, D_{\mathbf{k},\mathbf{q}}=\Delta_{\mathbf{k}}+\Delta_{\mathbf{q}}-\Delta-\delta=\nu_{\mathbf{k}}+\nu_{\mathbf{q}}-\nu_p-\nu_c$$

and $\delta=\nu_c-\omega_{ab}$. By using the Weisskopf-Wigner approximation, we obtain the set of linear

$$\frac{d}{dt}\tilde{A}_{\mathbf{k}}^{(1)}\simeq\left[-i(D_{\mathbf{k}}-\delta)-\tfrac{1}{2}\Upsilon^{(1)}\right]\tilde{A}_{\mathbf{k}}^{(1)}+i\Omega_c^{(1)}\tilde{B}_{\mathbf{k}}^{(1)}-\tfrac{1}{2}\sqrt{\Gamma^{(1)}\Gamma^{(2)}}f(r)\tilde{A}_{\mathbf{k}}^{(2)}(t), \tag{A5}$$

$$\frac{d}{dt}\tilde{A}_{\mathbf{k}}^{(2)}\simeq\left[-i(D_{\mathbf{k}}-\delta)-\tfrac{1}{2}\Upsilon^{(2)}\right]\tilde{A}_{\mathbf{k}}^{(2)}+i\Omega_c^{(2)}\tilde{B}_{\mathbf{k}}^{(2)}-\tfrac{1}{2}\sqrt{\Gamma^{(1)}\Gamma^{(2)}}f(r)^*\tilde{A}_{\mathbf{k}}^{(1)}(t), \tag{A6}$$

where

$$\sum_{\mathbf{q}}|g_{\mathbf{q}}^{(j)}|^2\int_0^t e^{-iD_{\mathbf{k},\mathbf{q}}(t-t')}\simeq\tfrac{1}{2}\Upsilon^{(j)}, \tag{A7}$$

$$\sum_{\mathbf{q}}g_{\mathbf{q}}^{(1)*}g_{\mathbf{q}}^{(2)}\int_0^t e^{-iD_{\mathbf{k},\mathbf{q}}(t-t')}\simeq\frac{1}{2}\sqrt{\Gamma^{(1)}\Gamma^{(2)}}f(r), \tag{A8}$$

with $\Upsilon^{(j)}=\Gamma^{(j)}-i\xi^{(j)}$, the Lamb shift $\xi^{(j)}$, $f(r)=g(r)+ih(r)$, where $g(r)$ gives the modified decay rates and $h(r)$ is the level shift factor [8] due to the collective effects.

The coupled equations can be solved by Laplace transform method. Assume that initially $C(0)=1$ and other coef-

ficients are zero, after a lengthy calculations, we obtain the steady state solution

$$C_{\mathbf{k},\mathbf{q}}(\infty)=i\left(\frac{i(\delta-\Delta_{\mathbf{q}})\frac{1}{2}\sqrt{\Gamma^{(1)}\Gamma^{(2)}}f(r)\Omega_c^{(1)}g_{\mathbf{q}}^{(2)}G_{\mathbf{k}}^{(1)}}{M_{\mathbf{q}}(\gamma_R-iD_{\mathbf{k},\mathbf{q}})}-\frac{\left\{i(\delta-\Delta_{\mathbf{q}})\left(\frac{\Gamma^{(2)}}{2}-i\Delta_{\mathbf{q}}\right)+|\Omega|^2\right\}\Omega_c^{(1)}g_{\mathbf{q}}^{(1)}G_{\mathbf{k}}^{(1)}}{M_{\mathbf{q}}(\gamma_R-iD_{\mathbf{k},\mathbf{q}})}\right)+(1\leftrightarrow 2), \tag{A9}$$

where $M_{\mathbf{q}}=\Pi_{j=1}^{4}(\Delta_{\mathbf{q}}-x_j)$ with $\{x_j\}=\{a_+^{(+)},a_-^{(+)},a_+^{(-)},a_-^{(-)}\}$, $a_{\pm}^{(\pm)}=\frac{1}{2}\delta-i\frac{1}{4}\Gamma^{(\pm)}\pm\tilde{\Omega}^{(\pm)}$ are the roots with $\tilde{\Omega}^{(\pm)}=\sqrt{|\Omega_c|^2-(\frac{1}{4}\Gamma^{(\pm)}-i\frac{1}{2}\delta)^2}$, $\gamma_R=\frac{1}{2}(\gamma_R^{(1)}+\gamma_R^{(2)})$ is the collective Raman decay rate with $\frac{1}{2}\gamma_R^{(j)}=\Sigma_{\mathbf{k}}\frac{|G_{\mathbf{k}}^{(j)}|^2}{s+iD_{\mathbf{k}}}$. The complex rates that depend on interatomic distance are $\Gamma^{(\pm)}=\Gamma[1\pm f(r)]$, where $f(r)$ is defined in the text.

For identical atoms, $\Gamma^{(2)}=\Gamma^{(1)}$. By neglecting the Lamb shifts $\Upsilon^{(1)}\simeq\Upsilon^{(2)}\simeq\Gamma$. We have verified that Eq. (A9) gives the known result [3] in the limit $f(r)\to 0$, for two independent atoms

$$C_{\mathbf{k},\mathbf{q}}(\infty)=\frac{i\sum_{j=1,2}\Omega_c^{(j)}g_{\mathbf{q}}^{(j)}G_{\mathbf{k}}^{(j)}}{\left[i\left(\frac{1}{2}\Gamma-i\Delta_{\mathbf{q}}\right)(\delta-\Delta_{\mathbf{q}})+|\Omega_c|^2\right](iD_{\mathbf{k},\mathbf{q}}-\gamma_R)}. \tag{A10}$$

The exact coefficient in Eqs. (6) and (7) are

$$\begin{aligned}K_{Aj}=2\wp_{ba,Aj}^{\parallel}&\left[\left(\frac{1}{ix_{Aj}^3}-\frac{1}{x_{Aj}^2}\right)+\sin^2\alpha_{Aj}\left(\frac{3}{2x_{Aj}^2}-\frac{3}{2ix_{Aj}^3}+\frac{1}{2ix_{Aj}}\right)\right]\\&+\wp_{ba,Aj}^{\perp}\left[\frac{1}{ix_{Aj}}+\frac{1}{x_{Aj}^2}-\frac{1}{ix_{Aj}^3}-\frac{1}{2}\sin^2\alpha_{Aj}\left(\frac{3}{x_{Aj}^2}-\frac{3}{ix_{Aj}^3}+\frac{1}{ix_{Aj}}\right)\right],\end{aligned} \tag{A11}$$

for dipole moment $\wp$ parallel ($\parallel$) and orthogonal ($\perp$) to the quantization axis, with $x_{Aj}=\nu r_{Aj}/c$ and α_{Aj} as the angles between A-j and the interatomic axis. The same expression for Q_{Bj} by the replacements $x_{Aj}\to y_{Bj}=\omega r_{Bj}/c$, $\wp_{ba,Aj}^{\parallel,\perp}\to\wp_{ca,Bj}^{\parallel,\perp}(B\text{-}j)$ and $\alpha_{Aj}\to\alpha_{Bj}$. The emission coupling factors K_{Aj}, Q_{Bj} are valid for both far and near fields [9].

[1] M. D'Angelo, M. V. Chekhova and Y. Shih, Phys. Rev. Lett. **87**, 013602 (2001).

[2] J. Xiong, D. Z. Cao, F. Huang, H. G. Li, X. J. Sun, and K. Wang, Phys. Rev. Lett. **94**, 173601 (2005).

[3] M. O. Scully and C. H. Raymond Ooi, J. Opt. B: Quantum Semiclassical Opt. **6**, S816 (2004).

[4] M. O. Scully and M. S. Zubairy, *Quantum Optics* (Cambridge University Press, Cambridge, 1997).

[5] M. O. Scully, Concepts Physics 2, 261 (2005).

[6] A very good description of dipole-dipole interaction can be found in the book by Z. Ficek and S. Swain, *Quantum Interference and Coherence* (Springer, Berlin, 2005); and monograph by G. S. Agarwal, in *Quantum Statistical Theories of Spontaneous Emission and Their Relation to Other Approaches*, edited by G. Hohler, Springer Tracts in Modern Physics, Vol. 70 (Springer, Berlin, 1974).

[7] For quantum regression approach, see A. K. Patnaik, G. S. Agarwal, C. H. Raymond Ooi, and M. O. Scully, Phys. Rev. A **72**, 043811 (2005); for Schrödinger's approach, see [9] or [3]; Heisenberg-Langevin approach will be presented elsewhere.

[8] R. H. Lehmberg, Phys. Rev. A **2**, 889 (1970).

[9] C. H. Raymond Ooi, A. K. Patnaik, and M. O. Scully, Proc. SPIE **5846**, 1 (2005).

[10] J.-T. Chang, J. Evers, M. O. Scully, and M. S. Zubairy, Phys. Rev. A **73**, 031803(R) (2006); J.-T. Chang, J. Evers, and M. S. Zubairy, *ibid.* **74**, 043820 (2006).